Proceedings of the 2nd International Conference on Computational Heat and Mass Transfer
COPPE/UFRJ – Federal University of Rio de Janeiro, Brazil, October 22-26, 2001

NUMERICAL SIMULATION OF ICE ACCRETION ON THE LEADING EDGE OF AERODYNAMIC PROFILES

RAFAEL A. DA SILVEIRA* AND CLOVIS R. MALISKA†

Abstract. The main goal of this work is the simulation of the ice accretion on the leading edge of aerodynamic profiles. The ice growth occurs when super cooled water droplets hit the airfoil surface during certain flying conditions. The well-known panel method is used to obtain the pressure coefficient and the velocity distribution on the surface. The local heat transfer coefficient is obtained by applying the Smith and Spalding method for the thermal boundary layer calculation and an ordinary differential equation is solved to compute the local Nusselt number. The ice accretion area and the collection efficiency are determined through the calculation of the water droplets trajectories hitting the surface. Each particle is considered a rigid sphere that doesn't affect the flow, but undergoes aerodynamic drag. An energy balance is done in each control volume on the body surface considering evaporative cooling, conduction, convection, phase change and kinetic heating. The amount of water that freezes inside the control volume is determined with a mass balance that comprehends evaporation, splashing caused by aerodynamic drag, droplets impingement and water shedding on the surface. Finally, the ice thickness computed by the mass balance is added to respective panel forming a new profile. The results obtained compare very well with the ones available in the literature. Computational strategies are being used in order to have a computer code able to be reusable and prone to addition of new improvements, keeping the original computational abstraction and efficiency.

Keywords: ice accretion, aerodynamics, lift coefficient.

1. Introduction. In certain flying conditions, the super-cooled water droplets contained in the clouds may freeze when impinging on the leading edge of the aircraft wings. The ice layer changes the airfoil shape and affects the lift characteristics of the plane, which may put in danger the flying operation. The atmospheric parameters which influences the ice accretion are velocity, temperature and pressure, and the meteorological parameters are the liquid water content, droplet diameter and the relative humidity. The model employed in this paper consists of six basics steps: definition of the airfoil geometry, potential flow solution, boundary layer calculation, determination of water droplets trajectories impinging the airfoil surface, heat and mass balances and the modification of the airfoil geometry due to the ice accretion. The calculation procedure marches in time, beginning with the velocity calculation for each panel on the airfoil geometry. In each time step the thickness of ice deposited in each panel is added to the geometry. With this new geometry a new calculation is performed marching in time until the desired icing time is reached.

2. Mathematical Formulation. This section describes the mathematical model used to calculate the ice accretion. The six major steps of the calculation procedure are shown. For each step, only the most important equations are provided.

2.1. Geometry Generation. The first step is the definition of the geometry to be analyzed. The geometry usually comes from a CAD system, furnishing the coordinates of each panel defining the surface. In this paper cylinders were used to validate some steps of the methodology and NACA 4 and 5 digits series of airfoils were used (Mason, 2000) to calculate ice accretion profiles. Grid generation is not necessary in this model, because the flow solution is obtained with the panel method (Hess and Smith, 1967).

2.2. Flow Solution. The pressure coefficient, the velocity distribution and the position of the stagnation point are obtained with the potential flow calculation using the panel method. The panel method is a very efficient method due its robustness, simplicity and minor requirements in computer time. It is, however, limited to ice accretion that does not form ice horns. The governing equation of the potential flow is the Laplace's equation, given by

$$\nabla^2 \phi = 0 \tag{2.1}$$

* Mechanical Engineering Department – UFSC, PO Box 476, 88040-000 Florianópolis SC, Brazil silveira@sinmec.ufsc.br
† Mechanical Engineering Department – UFSC, PO Box 476, 88040-000 Florianópolis SC, Brazil maliska@sinmec.ufsc.br

where ϕ is the potential velocity function. This equation is solved with the panel method, which consists in dividing the surface in several segments, named "panels", joining a discrete set of coordinates, and distribute sources and vortices (elementary flows) over these segments. This method is widely used and it will not be presented here. A complete description of it can be found in Mason (2000) and Silveira (2001), among many other sources.

2.3. Boundary Layer Calculation. Knowing the potential flow it is necessary to calculate the thermal boundary layer to obtain the local heat transfer coefficient, required for the heat balance on the airfoil surface. The ice roughness caused by the impingement of the droplets on the surface is believed responsible for the turbulence in this flow. Therefore, a turbulence model is used in order to take into account this effect. The transition from laminar to turbulent is calculated by (Wright, 1995)

$$\mathrm{Re}_k = U_k k_s / \nu \tag{2.2}$$

where U_k is the velocity at the roughness height and k_s is the roughness height in each location. The transition is assumed when Re_k is greater than 600. In the laminar region, the Smith-Spalding's method (Schlichting, 1979) is used. The thermal boundary layer thickness at the center of each panel, in this case, is given by

$$\delta_t^{\,2} = \frac{46.72\nu}{U^{2.87}} \int_0^x U^{1.87} dx \tag{2.3}$$

where x is the surface coordinate measured from the stagnation point. The local Nusselt number can be obtained from

$$\mathrm{Nu}_c(x) = 2c / \delta_t \tag{2.4}$$

For turbulent flow, the local Nusselt number is given (Wright, 1995) by

$$\mathrm{Nu}_c(x) = \frac{(C_f' / 2)\mathrm{Re}_x \mathrm{Pr}}{\mathrm{Pr}_t + (C_f' / 2)^{0.5}[0.52(\mathrm{Re}_{k,r})^{0.45} \mathrm{Pr}^{0.8}]} \tag{2.5}$$

where

$$\mathrm{Re}_{k,r} = u_r k_s / \nu \tag{2.6}$$

and

$$u_r = U(C_f' / 2)^{0.5} \tag{2.7}$$

The skin-friction coefficient, C_f', is obtained from

$$C_f' / 2 = \{0.41 / [\log(864\delta_2 / k_s + 2.568)]\}^2 \tag{2.8}$$

and the momentum thickness is given by

$$\delta_2 = \frac{0.36\nu^{0.2}}{U^{3.29}} \left(\int_0^x U^{3.86} dx \right)^{0.8} \tag{2.9}$$

The model used in (Wright, 1995) considers the roughness height as a function of the wetness factor that, by its turn, is a function of the contact angle of the droplet on the surface. In this work the roughness height is considered constant along the surface and its value is an input of the program. The consequences of this simplification are discussed later.

2.4. Droplets Trajectories. The position where a droplet impinges on the body surface must be known for the calculation of the impingement limits and of the local collection efficiency. Therefore, the droplets trajectories must be calculated. In this case, a droplet is considered as a small sphere that doesn't affect the flow but undergoes aerodynamic drag, as shown in Fig. 1.

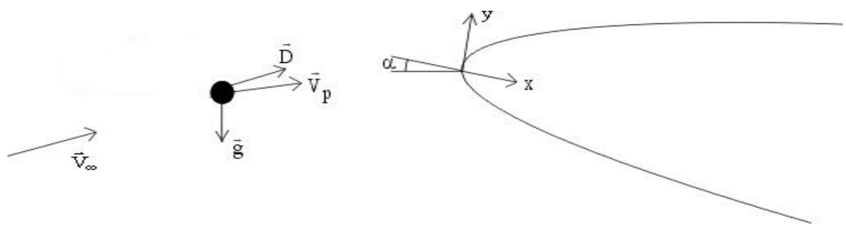

Fig. 1: forces acting on the water drop

The equations of motion for the droplets are

$$m\ddot{x} = -D\cos\gamma + mg\sin\alpha \tag{2.10}$$

$$m\ddot{y} = -D\sin\gamma - mg\cos\alpha \tag{2.11}$$

where

$$\gamma = \tan^{-1}[(\dot{y}_p - v)/(\dot{x}_p - u)] \tag{2.12}$$

and $(\dot{x}_p, \dot{y}_p)$ are the components of the droplet velocity, and (u, v) are the components of flow velocity at the droplet position. The drag is defined as

$$D = C_d \rho_a V^2 A_p / 2 \tag{2.13}$$

with

$$V = \left[(\dot{x}_p - u)^2 + (\dot{y}_p - v)^2\right]^{0.5} \tag{2.14}$$

and A_p is the projected area of the droplet. The drag coefficient (White, 1991) is given by

$$C_d = \frac{24}{Re_{d_p}} + \frac{6}{1 + (Re_{d_p})^{0.5}} + 0.4 \tag{2.15}$$

where

$$Re_{d_p} = V d_p / \nu \tag{2.16}$$

and d_p is the diameter of the droplet

The impingement limits, the limiting trajectories hitting the body surface, are calculated with an iterative process. For the upper impingement limit, it is first chosen a trajectory that impinges the body. Next, it is chosen a trajectory passing above the body not hitting the surface. The trajectory lying half-away between these two ones is then calculated. If it impinges the body, it will be the new trajectory impinging the body. Otherwise, it will be the new trajectory that passes above the body and a new half-away trajectory is calculated. The process is repeated until the distance between the initial positions of two trajectories is less than a specified value. For the lower surface, the process is the same.

The local collection efficiency represents the fraction of the liquid water content (LWC) captured by that location of the surface.

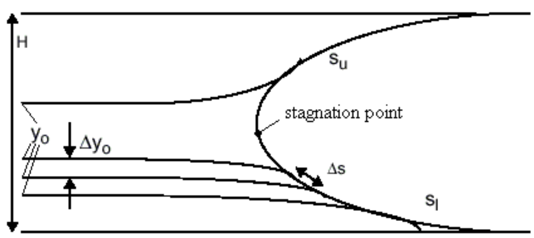

Fig. 2: impingement limits and initial position of trajectories

According to Fig. 2, the value of the local collection efficiency, β, is given by

$$\beta = \Delta y_0 / \Delta s \tag{2.17}$$

where ‘s’ is the position on the surface measured from de stagnation point.

2.5. Thermodynamic Model. To calculate the freezing rates, heat and mass balances are carried out in control volumes located at the surface between the impingement limits. The surface is always considered to be the surface of the ice. Of course, if there is no ice formation, the surface is the body geometry. When the droplets impinge the body, a thin layer of water is formed on the surface. Therefore, the control volumes will have a very small thickness and the unknown, $T_{s,}$ obtained from the heat balance, is the temperature of the water film that will result in the ice growth rate. The balances begin at the panel next to stagnation point and march along the surface for each segment on upper and lower surfaces.

2.5.1. Heat Balance. The heat fluxes can be sketched as shown in Fig. 3. Only the final expression is written. Details can be found in (Wright, 1995) and (Silveira, 2001).

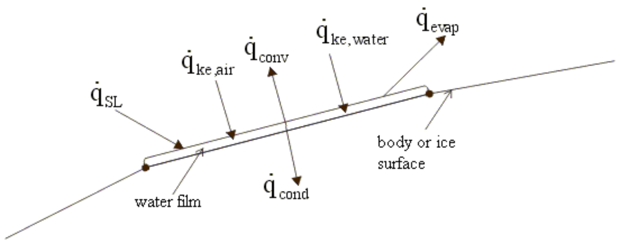

Fig. 3: heat balance

The energy balance reads

$$\dot{q}_{evap} + \dot{q}_{cond} + \dot{q}_{conv} + \dot{q}_{ke,air} + \dot{q}_{ke,water} + \dot{q}_{SL} = 0 \tag{2.18}$$

where the heat lost by **evaporation** of water on the surface is given by

$$\dot{q}_{evap} = \dot{m}_{evap} . L_v \tag{2.19}$$

where

$$\dot{m}_{evap} = \frac{h_c}{c_{p,air}} \frac{MW_{water}}{MW_{air}} L^{-2/3} \left[\frac{P_{v,\infty}}{P_\infty} r_h - \frac{P_{v,s}}{P_o} \frac{T_o}{T_s} \left(\frac{P_o}{P_e} \right)^{1/\gamma} \right] \tag{2.20}$$

The heat lost by **conduction** into the body is modeled by considering the body as a 1D semi-infinite solid and assuming that the surface temperature exhibits an instantaneous temperature change at initial time, given by the recovery temperature. Therefore, the conduction term is given by

$$\dot{q}_{cond} = -k(T_{rec} - T_s)/(\pi\alpha t)^{0.5} \tag{2.21}$$

where

$$T_{rec} = T_\infty \{1 + r[(P/P_o)^{(1-\gamma)/\gamma} - 1]\} \tag{2.22}$$

is the recovery temperature and r is the recovery factor given by $Pr^{1/2}$ for the laminar region and $Pr^{1/3}$ for the turbulent region.

Sensible and latent heat are accounted by considering two quantities that must be added in the balance: the water from the impingement of the droplets and the water that flows over the surface entering the control volume (runback water). If none of the water freezes, there is only sensible heat for the water to reach its final temperature T_S. This is expressed, for the water from impingement and for the runback water, respectively, by

$$\dot{q}_{SL} = \dot{m}_{imp} c_{p,water} (T_s - T_\infty) \tag{2.23}$$

$$\dot{q}_{SL} = \dot{m}_{rb,in} c_{p,water} (T_s - T_{rb}) \tag{2.24}$$

If part of the water freezes, there is sensible heat for the water to reach the melting temperature (T_{mp}= 273.15 K) and latent heat for the solidification. For the two quantities, the amount of sensible and latent heat is given by

$$\dot{q}_{SL} = \dot{m}_{imp} \left[c_{p,water} (T_\infty - T_{mp}) + \left(c_{p,ice} T_{mp} \left(1 - \frac{\rho_{ice}}{\rho_{water}} \right) + c_{p,ice} \Delta T_m + L_f \right) \frac{T_{mp} + \Delta T_m - T_s}{\Delta T_m} \right] \tag{2.25}$$

$$\dot{q}_{SL} = \dot{m}_{rb,in} \left[c_{p,water} (T_{rb} - T_{mp}) + \left(c_{p,ice} T_{mp} \left(1 - \frac{\rho_{ice}}{\rho_{water}} \right) + c_{p,ice} \Delta T_m + L_f \right) \frac{T_{mp} + \Delta T_m - T_s}{\Delta T_m} \right] \tag{2.26}$$

The term $(T_{mp} + \Delta T_m - T_s) / \Delta T_m$ appearing in the last equations is defined as the freezing fraction, which is replaced by the temperature, since the balance is carried out to determine the value of T_S. The freezing fraction, N_f, is the fraction of liquid water in the control volume that freezes. If $N_f = 0$, none of the water freezes. If $N_f = 1$, all of the water freezes and if $0 < N_f < 1$, a part of the water freezes.

Finally, if all of the water freezes, there are three terms to be accounted for: sensible heat for the water to reach the melting temperature, latent heat for phase change and sensible heat for the ice to reach its final temperature T_S. For the water from impingement and from runback water, the fluxes are, respectively

$$\dot{q}_{SL} = \dot{m}_{imp} \left[c_{p,water} (T_\infty - T_{mp}) + c_{p,ice} T_{mp} \left(1 - \frac{\rho_{ice}}{\rho_{water}} \right) + c_{p,ice} (T_{mp} + \Delta T_m - T_s) + L_f \right] \tag{2.27}$$

$$\dot{q}_{SL} = \dot{m}_{rb,in} \left[c_{p,water} (T_{rb} - T_{mp}) + c_{p,ice} T_{mp} \left(1 - \frac{\rho_{ice}}{\rho_{water}} \right) + c_{p,ice} (T_{mp} + \Delta T_m - T_s) + L_f \right] \tag{2.28}$$

The **kinetic heating** is due to two reasons: kinetic heating from the air and kinetic heating from the impinging water droplets. These fluxes are represented by (Wright, 1995)

$$\dot{q}_{ke,air} = h(T_{rec} - T_\infty) \tag{2.29}$$

$$\dot{q}_{ke,water} = \dot{m}_{imp} V_\infty^2 / 2 \tag{2.30}$$

Finally, the **convection** flux is given by

$$\dot{q}_{conv} = h(T_\infty - T_s) \tag{2.31}$$

Inserting the equations for the fluxes calculation in Eq. (2.18), the resulting expression is a non-linear equation for T_S for each panel, which is solved using the Newton-Raphson method. Recall that only one of the three pairs of equations of the sensible and latent heat fluxes is used, depending on the value of the freezing fraction.

2.5.2. Mass Balance. When the freezing fraction is obtained, the mass balance is carried out for determining the rate of freezing water in each segment of the surface. Considering the film of water as a small control volume, the mass balance can be sketched as shown in Fig. 4

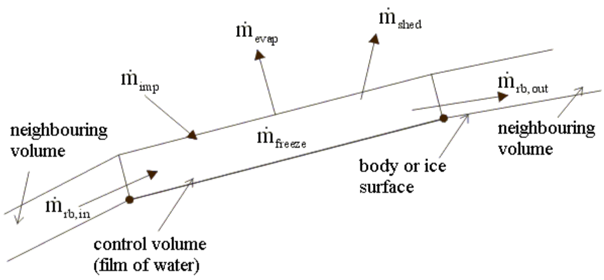

Fig. 4: mass balance

The **evaporation** mass flux, $\dot{m}_{evap}$, was already determined in the evaporation heat flux, and is given by Eq. (2.20). The **impingement** water flux can be also computed independently, by using the expression given by (Sherif and Pasumarthi, 1995)

$$\dot{m}_{imp} = \beta V_\infty LWC \tag{2.32}$$

The water **shedding,** due to aerodynamic force, is calculated based on the Weber number. An experimental expression is used to find the amount of water shedding (Wright, 1995). If the Weber number, defined as $W_e = \rho U^2 L / \sigma$, is larger than a critical value (500 is used), the mass rate lost due to the shedding is given by

$$\dot{m}_{shed} = [(W_e - W_{e,c}) / W_e](\dot{m}_{imp} + \dot{m}_{rb,in}) \tag{2.33}$$

where $\dot{m}_{rb,in}$ is the runback water from the previous panel.

Finally, the **freezing water** rate on each panel can be written as

$$\dot{m}_{freeze} = N_f (\dot{m}_{imp} + \dot{m}_{rb,in} - \dot{m}_{shed} - \dot{m}_{evap}) \tag{2.34}$$

and all of water that do not freeze is considered to flow into the next control volume (panel) and is given by

$$\dot{m}_{rb,out} = (1 - N_f)(\dot{m}_{imp} + \dot{m}_{rb,in} - \dot{m}_{shed} - \dot{m}_{evap}) \tag{2.35}$$

After computing the value of freezing rate, the ice thickness, h, can be calculated by specifying a time step and using the following expression

$$h = \dot{m}_{freeze} \Delta t / \rho_{ice} \tag{2.36}$$

3. Validation and Results. This section presents some of the results obtained with the model. The flow validation of the flow solution and the trajectories calculation were validated using simple geometries. To validate the thermodynamic model of ice accretion, aerofoil profiles were used.

3.1. Flow Past a Cylinder. The **velocity profile** of the potential flow over a cylinder, obtained with panel method was compared with the analytical solution shown in (Schlichting, 1979). Figure 5 shows the velocity on the body for a free stream velocity of 20 m/s, where x is the angle measured from the stagnation point in the upper surface. The heat transfer coefficient was computed using a constant roughness distribution. The results for some values of roughness, compared with the variable distribution found in (Wright, 1999) are shown in Fig. 6. The diameter of cylinder is 0.1524 m and the free stream velocity is 90 m/s. The coordinate x/c is the surface coordinate measured from stagnation point. The plot shows that for a roughness of 0.05 mm the flow is laminar along surface. For larger values, transition occurs closer and closer to stagnation point (x/c = 0) as the roughness increases. The curves for 0.1 mm and 0.2 mm show a reasonable agreement with data available in Wright (1999).

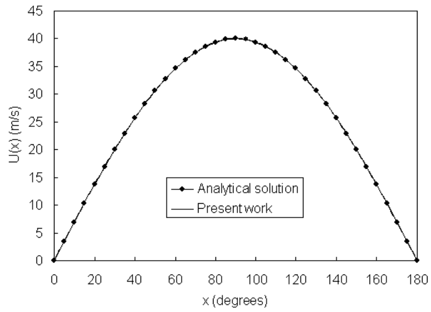

Fig. 5: potential velocity on a cylinder

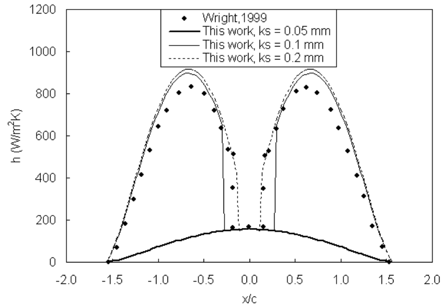

Fig. 6: heat transfer coefficient

The local collection efficiency validation is done with the same case used to check the heat transfer coefficient. The droplet diameter considered is 20μm and Fig. 7 shows the data computed in this work comparing to the data of (Wright, 1999).

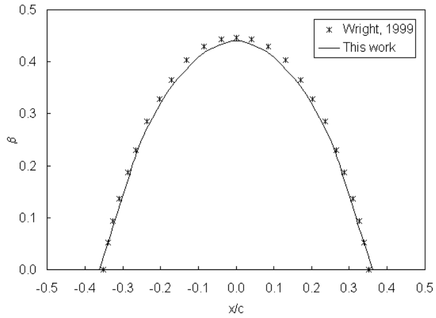

Fig. 7: local collection efficiency

3.2. Ice accretion on airfoils. The ice profiles calculated were compared with the results from experimental work and from two other sources: the code Lewice 1.6, developed at NASA, and the code from the Defense Research Agency-England (DRA). The results that follow are for the NACA 0012 airfoil, available in (Wright et al, 1997).

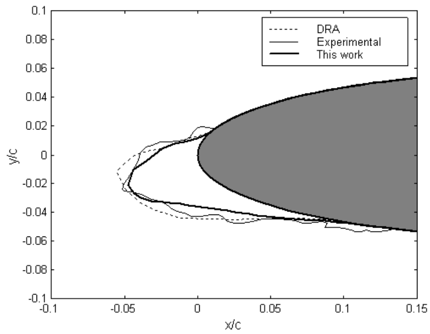

Fig. 8: Case 1: Exp., DRA and this work

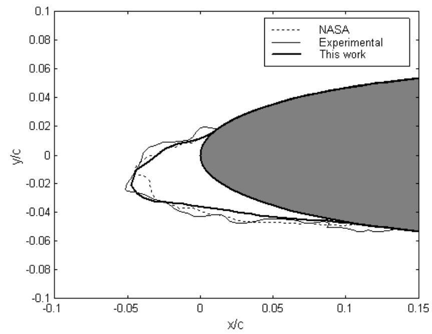

Fig. 9: Case 1: Exp., Lewice and this work

Figs. 8 and 9 show the ice profile for the following conditions: Case 1: c = 0.5334 m; $\alpha = 4°$; V_∞ = 58.1 m/s; P_∞ = 95610 N/m^2; T_∞ = 245.2 K; d_p = 20 μm; LWC = 1.3 g/m^3 and time = 480 s and Case 2 are: c = 0.5334 m; $\alpha = 4°$; V_∞ = 93.8 m/s; P_∞ = 92060 N/m^2; T_∞ = 242.5 K; d_p = 20 μm; LWC = 1.05 g/m^3 and time = 372 s, with the results shown in Figs. 10 and 11. For both conditions the results agree well with the numerical ones. When compared with the experimental results, all the numerical computations shows a local discrepancy, but with a good overall agreement for the ice profile. Results for other geometries including the analysis of the influence of the meteorological, atmospheric and geometrical parameters can be found in (Silveira, 2001).

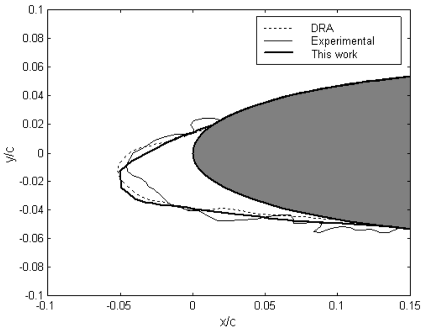

Fig. 10: Case2: Exp., DRA and this work

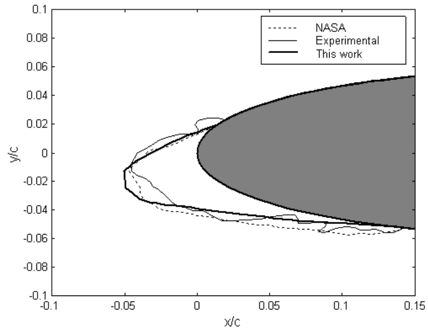

Fig. 11: Case 2; Exp., Lewice and this work

4. Conclusions. The development of a methodology for calculating ice accretion in aerodynamic profiles was developed. The model is the first step toward the development of a more general methodology able to deal with the real problem of ice accretion in aircraft wings. The several step of the procedure were validated and the results of ice deposition for two different conditions show good agreement with the other numerical and experimental results. The code was designed such that flow results from Navier-Stokes solvers can easily be given as input.

5. Symbols

c	- Chord [m];
d_p	- Droplet diameter [m];
h, h_c	- Heat transfer coefficient[W/m^2·K];
k_s	- Roughness height [m];
L	- Lewis number = $k/\rho c_p D_{AB}$ [dimensionless];
L_f	- Latent heat of fusion of water [J/kg];
L_v	- Latent heat of vaporization of water [J/kg];
MW	- Molecular weight [kg/kmol];
$\dot{m}$	- Mass flux [kg/m^2·s];
P_v	- Vapor pressure [N/m^2];
$\dot{q}$	- Heat flux [W/m^2];
r_h	- Relative humidity of air [dimensionless];

subscripts

cond	- Conduction;
conv	- Convection;
e	- Edge of boundary layer;
evap	- Evaporation;
freeze	- Freezing mass;
imp	- Impinging water;
ke, air	- Kinetic heating due to air;
ke, water	- Kinetic heating due to water;
o	- Stagnation or total property;
rb	- runback water;
SL	- Sensible and latent heats;
shed	- water shedding;

REFERENCES

[1] HESS, J. L. and SMITH, A. M. O. Calculation of potential flow about arbitrary bodies. *Progress in Aeronautical Sciences*, 8 (1967), 1-138.

[2] MASON, W. H. *Applied Computational Aerodynamic Text/Notes*. URL <http://www.aoe.vt.edu/facult/Mason_f > May 2000.

[3] SCHLICHTING, H. *Boundary Layer Theory*. McGraw-Hill, 1979.

[4] SHERIF, S. A. and PASUMARTHI, N. Local heat transfer and ice accretion in high speed subsonic flow over an airfoil. AIAA Paper 2104 (1995).

[5] SILVEIRA, R. A.. Numerical Simulation of Ice Accretion on the Leading Edge of Aerodynamic Profiles. M.Sc Dissertation, Federal University of Santa Catarina, Florianópolis, SC, BRAZIL, 2001. IN PORTUGUESE.

[6] WHITE, F. M., V*iscous Fluid Flow*. McGraw-Hill, 1991.

[7] WRIGHT, W. B. Users manual for the improved NASA Lewis ice accretion code Lewice 1.6. *NASA CR - 198355* (1995).

[8] WRIGHT, W. B. Users manual for the NASA Glenn ice accretion code Lewice version 2.0. *NASA CR - 209409* (1999).

[9] WRIGHT, W. B., GENT, R. W. and GUFFOND, D. DRA/NASA/ONERA collaboration on icing research part II – Prediction of airfoil ice accretion. *NASA CR - 202349* (1997).